

04
Investigation of the surface temperature in contact with plasma by two-color pyrometry

© A.V. Voronin,¹ V.Yu. Goryainov,^{1,2} A.A. Kapralov,¹ V.A. Tokarev,¹ G.Yu. Sotnikova¹

¹ Ioffe Institute, St. Petersburg, Russia

² Peter the Great Saint-Petersburg Polytechnic University, St. Petersburg, Russia

E-mail: vgoryainov@mail.ioffe.ru

Received December 1, 2022

Revised February 14, 2023

Accepted February 21, 2023

A high-speed two-color pyrometer has been developed that allows measuring the intensity of thermal radiation in temperature range of 100–3500°C with 2 μs time resolution. The analysis of main factors affecting the measurement of surface temperature in the conditions of its interaction with plasma is carried out. It is shown that at plasma temperature of more than 10 eV and moderate particles density, the wall plasma can be considered transparent to thermal radiation. Experimental studies on non-contact measurement of temperature of surface interacting with plasma on Globus-M2 tokamak and plasma gun test bench have been carried out. Sawtooth temperature oscillations were detected on the wall of tokamak chamber near the exit of outer separatrix branch. The period of these flashes was 3–4 ms, and duration was 2 ms. The maximum wall temperature measured by a high-speed pyrometer exceeded temperature measured by infrared camera. Front surface temperature measurements of W-Li sample were carried out at plasma gun test bench under conditions of deuterium plasma jet cyclic action under loads simulating regimes of plasma current disruption in tokamak. The sample temperature reached more than 3000°C during ~ 1 ms. The thermal conductivity of the sample degraded with an increase in number of plasma exposure cycles, which was expressed in progressive decrease in target cooling rate after the pulse. Using a high-speed pyrometer, it is proposed to control the formation of heat-insulating foils on surface interacting with plasma.

Keywords: two-color pyrometer, thermal radiation, surface temperature, materials irradiation.

DOI: 10.21883/TP.2023.05.56063.262-22

Introduction

Currently, applied and fundamental research aimed at studying pulsed interaction of plasma with the surface is actively carried out. The material is subjected to high thermal loads (up to hundreds GW/m²), which can be evaluated by temperature control [1,2]. The most effective and in-demand diagnostics is high-speed contactless pyrometry in such conditions [3].

It is known [4] that the spectral intensity (spectral power density) of thermal radiation of an object with a radiation coefficient of ε(λ) is described by Planck’s formula:

$$I(\lambda, T) = \varepsilon(\lambda) \frac{2\pi hc^2}{\lambda^5} \frac{1}{e^{\frac{hc}{\lambda kT}} - 1} \left[\frac{W}{m^2 \cdot m} \right], \quad (1)$$

where *T* — absolute temperature in K, *c*, *h*, *k* — speed of light, Planck and Boltzmann constants in SI, respectively.

Absolute measurements of radiation intensity, depending on the problem being solved, are conducted in different regions of the thermal radiation spectrum on one or several spectral lines of different widths when using optical pyrometry methods in various fields of science and technology [5]. The highest measurement accuracy is provided by color pyrometers implementing spectral ratio method ([5] and references therein). The spectral ratio method consists in finding the surface temperature of an

object from ratio of intensities of its thermal radiation at two narrow spectral wavelengths located close to each other. This approach makes it possible to significantly reduce the basic methodological error of optical pyrometry associated with the lack of accurate knowledge about magnitude of the radiation coefficient of the object under study and its possible changes in the measurement process. A slight difference in values ε(λ₁) and ε(λ₂) will not affect the pyrometer readings with the correct choice of wavelengths (λ₁, λ₂), on which the absolute values of the thermal radiation intensity of the object are measured. The ratio of radiation intensity signals will depend only on relative parameter ε(λ₁)/ε(λ₂), which, with correct choice of measurement wavelengths, can be considered constant (slightly variable), and the correct result of temperature measurement can be obtained without precise knowledge of absolute value of object’s radiation coefficient. This paper presents the results of an experimental study of W-Li material. The data known from the reference literature for various metals [6] allow expecting that values of radiation coefficient of material, ε(λ₁) and ε(λ₂), for the spectral measurement range 3–4 μm will not only be close, but also more importantly, their ratio, ε(λ₁)/ε(λ₂), will vary slightly over a wide temperature range up to 30,000°C.

Dependence of the value of thermal radiation intensity recorded by pyrometer on the distance is same for both pyrometer receivers, therefore it also does not affect the signal ratio. The shape of measured object and changes in transparency (dustiness of optical elements, the viewing window of vacuum chamber, gas contamination) of intermediate medium, if they do not have abnormal absorption lines in the region of narrow spectral lines of the pyrometer, equally affect signals of both receivers, leaving their ratio unchanged. Two-color pyrometers are also insensitive to lateral illumination from large-sized objects, the presence of small opaque objects in the field of view of pyrometer, etc. [4]. This principle of temperature measurement allows eliminating disadvantages inherent in devices (for example, infrared cameras) operating in same spectral range. In the present work, the temperature was measured from the ratio of recorded thermal radiation powers of object on nearby spectral lines in the infrared region of the spectrum.

In two-color pyrometry, the ratio of two signals is $I_1(\lambda_1)/I_2(\lambda_2)$, provided the sensitivity band of photodetectors used is sufficiently narrow (in optics, the condition of quasi-monochromaticity is considered to be fulfillment of condition $\Delta\lambda/\lambda_{\max} \leq 0.1$, where $\Delta\lambda$ — the width of spectral characteristic of a photodetector with a maximum sensitivity at wavelength λ_{\max}) can be recorded using Planck's radiation law, taking into account relative parameter $\varepsilon(\lambda_1)/\varepsilon(\lambda_2)$, transmission of intermediate medium and the parameters of optical and electrical circuits of the pyrometer combined into a single conversion coefficient A, according to the formula (2):

$$\frac{I_1(\lambda_1)}{I_2(\lambda_2)} = A \left(\frac{\lambda_2}{\lambda_1} \right)^5 \frac{e^{\frac{hc}{k\lambda_2 T}} - 1}{e^{\frac{hc}{k\lambda_1 T}} - 1}, \quad (2)$$

where the coefficient A is determined by calibrating pyrometer to a source with a known temperature under conditions identical to intended experiment.

The rationale for using a quasi-monochromatic model of pyrometer transfer function based on spectral narrowband photodiodes of the mid-IR range used by us is presented in the work [7].

1. Pyrometer device

A two-color IR pyrometer developed at the Ioffe Institute was used to record intensity of thermal radiation of elements facing the plasma [8]. Block diagram and appearance of pyrometer are shown in Fig. 1. The main element of pyrometer was a two-wave photodiode (PD), which comprised sandwich structure 5.1/5.2 with an active region having a transverse size of 0.3 mm. The region of spectral sensitivity to radiation of the first layer was $\Delta\lambda_1 = 3.25 \pm 0.15 \mu\text{m}$ and was practically transparent to radiation at other wavelengths. The second layer was sensitive to radiation in spectral region $\Delta\lambda_2 = 4.05 \pm 0.2 \mu\text{m}$. As you can see, the condition of quasi-monochromaticity of photodetector is fulfilled for

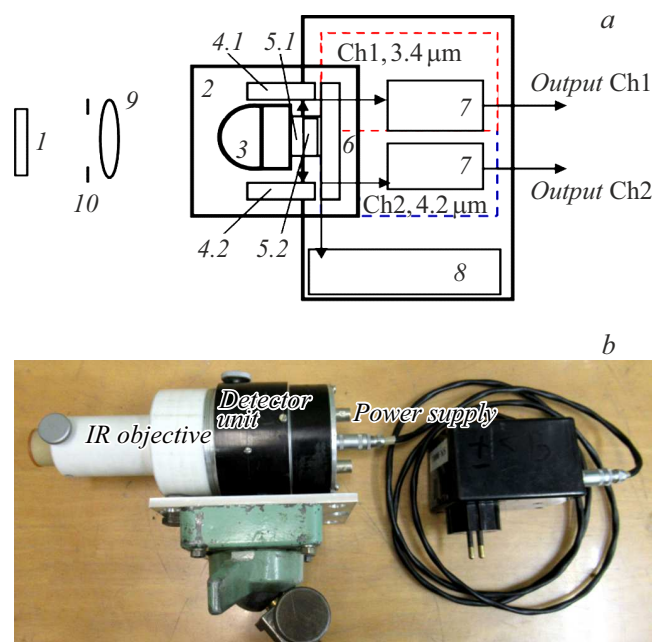


Figure 1. *a* — pyrometer block diagram: 1 — heated object, 2 — sealed housing, 3 — immersion Si-lens, 4.1/4.2 — photodiode current amplifier/converter, 5.1/5.2 — IR photodiodes, 6 — TEC, 7 — photodiode signal amplification circuit, 8 — TEC control microprocessor, 9 — additional IR (SeZn) lens, 10 — aperture; *b* — appearance of the pyrometer.

both photodiodes, which allows using the expression (2) with further calculations. Each layer of the sandwich structure had its own output. Thus, there was a spectral separation of radiation from the object into two channels: channel Ch1 recorded radiation in the spectral range $\Delta\lambda_1$, and channel Ch2 recorded radiation in the spectral range $\Delta\lambda_2$. PD currents were measured and converted into voltage signals Output Ch1, Ch2 by independent PD circuits in each of channels (4.1/4.2 in Fig. 1, *a*) installed in a sealed enclosure 2 in close proximity from PD chips and subsequent amplification circuits due to which the pyrometer's performance was not worse than $2 \mu\text{s}$ for each of the channels. The sandwich structure chips 5.1/5.2 were installed on a Peltier thermoelement (PTE, 6), which is an element of the design of the PD housing, which was necessary to stabilize their characteristics. The temperature of the PD and the circuits of the pre-amplifiers/current converters was stabilized at $(20 \pm 2)^\circ\text{C}$ and was maintained with an accuracy of $\pm 0.1^\circ\text{C}$, which made it possible to ensure stability of PD characteristics with minimal power consumption of the PTE. PD temperature of stabilization was controlled by a microprocessor 8. The spectral sensitivity of a photodiode with a double wavelength is shown in Fig. 2. The optical scheme of pyrometer, placed at a distance of 1.5 m from the object ensured the measurement of the intensity of thermal radiation from a surface with a diameter of ~ 20 mm in the temperature range $100\text{--}3500^\circ\text{C}$. The time resolution of pyrometer was $2 \mu\text{s}$.

Primary calibration of pyrometer was performed on the test bench shown in Fig. 3. The radiation source was a stainless steel screen placed inside the muffle furnace. Temperature readings of the screen surface were measured using a calibrated thermocouple, which were taken as true values of its temperature. During heating process, simultaneously with the thermocouple readings, pyrometer readings were recorded in increments of 10°C . Intensity of radiation incident on the sensor was set within the dynamic range of the PD using a diaphragm. Then, the experimental points were interpolated with a functional dependence (2) using the Origin software to determine conversion coefficient A , taking into account all technical characteristics of this particular pyrometer. Figure 4 shows experimental points together with resulting interpolation function of the form (2) with coefficient $A = 2.4$. Data obtained as a result of calibration allowed estimating the error of quasi-monochromatic model used to describe the transfer function of pyrometer. The error was 2.9% in temperature range from 50 to 800°C (maximum heating temperature of the object that could be realized in muffle furnace). The use of a functional dependency of the type (2) allows not only for interpolation of transfer function of

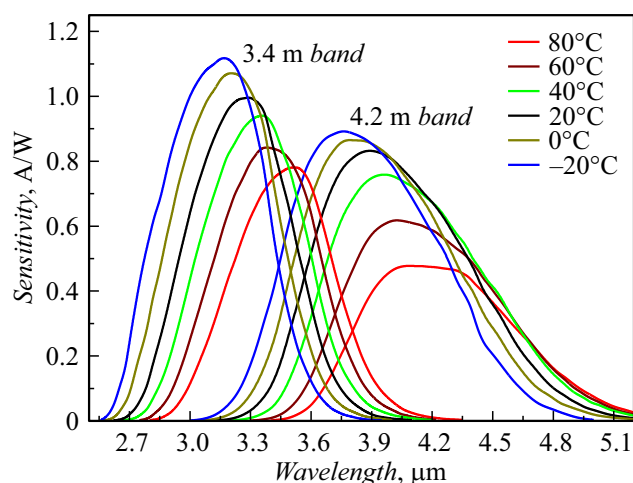


Figure 2. Spectral sensitivity of double wavelength PD $3/4\mu\text{m}$.

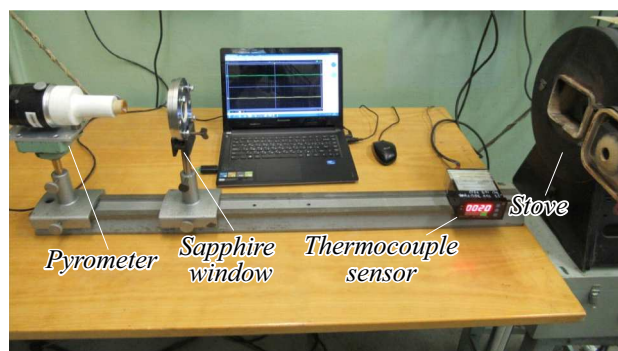


Figure 3. Pyrometer calibration test bench using the method of sample heating in a muffle furnace.

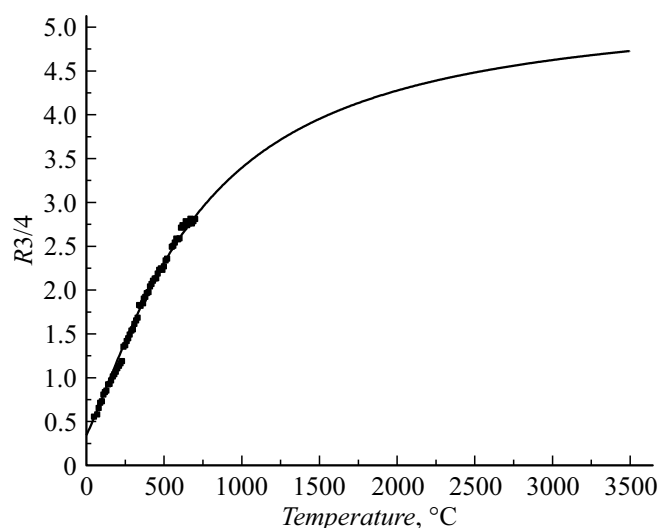


Figure 4. Dependence of the ratio of two pyrometer signals on temperature, calculated according to Planck formula, taking into account of device calibration.

the pyrometer to the region of higher temperatures, but also for periodic calibration of pyrometer at one arbitrary reference temperature point to clarify the value of the coefficient A when measurement conditions change. In particular, the pyrometer was periodically calibrated when sapphire windows used in the vacuum chamber before and after plasma experiments were installed in its optical circuit. The effect of change in transmission coefficient of the window on the pyrometer readings was not detected.

2. Factors influencing the interpretation of temperature measurements

The interpretation of obtained measurement and calculation results was complicated by not fully studied properties of resulting plasma near irradiated surface. Thus, the radiation of atomic hydrogen and carbon lines in the Globus-M2 tokamak was not detected on plateau of the current. These lines burned out during the rise and fall of the current. The glow of CIII-CVI lines was observed on the plateau. Therefore, taking into account the absence of intense radiation lines in the $3\text{--}4\mu\text{m}$ region, it can be assumed that recombination and bremsstrahlung radiation of wall plasma can have the most possible effect on measurement error. Figure 5 shows the results of calculations of the dependence of the spectral power density of recombination E_{rec} - and bremsstrahlung E_{bre} -radiation on the temperature of hydrogen plasma for two different densities: $n = 10^{19}\text{ m}^{-3}$ and $n = 10^{20}\text{ m}^{-3}$. The calculations are performed according to the formulas (1) and (3), (4),

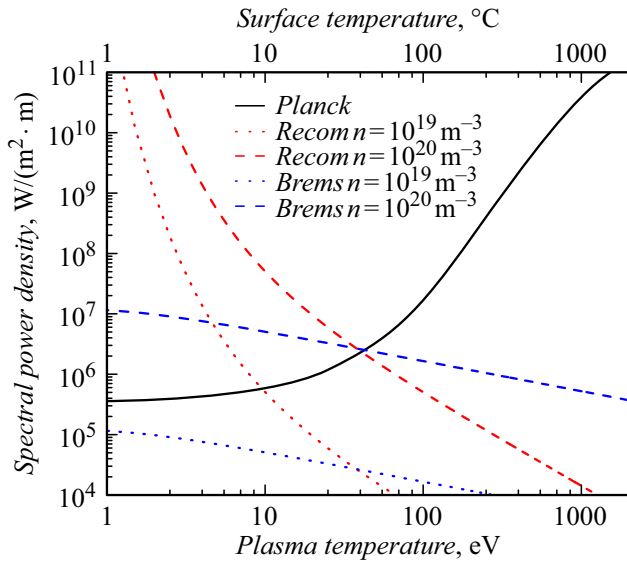


Figure 5. Dependence of the power density of recombination, bremsstrahlung and thermal radiation on the temperature of the plasma and the wall, respectively. The optical thickness of plasma layer in the Globus-M2 tokamak was 1 m.

which are presented in [9]:

$$E_{\text{rec}} = \frac{5.1 \cdot 10^{-27} n^2}{\lambda^2 T^{3/2}} \exp\left(-\frac{12400}{T} \left(\frac{1}{\lambda} - \frac{1}{940}\right)\right), \left[\frac{\text{W}}{\text{cm}^3 \text{Å}}\right], \quad (3)$$

$$E_{\text{bre}} = \frac{1.9 \cdot 10^{-28} n^2}{\lambda^2 T^{1/2}} \exp\left(-\frac{12400}{\lambda T}\right), \left[\frac{\text{W}}{\text{cm}^3 \text{Å}}\right], \quad (4)$$

where n — plasma density, $[\text{cm}^{-3}]$, T — plasma temperature, $[\text{eV}]$, λ — wavelength, $[\text{Å}]$.

The same graph shows the dependence of spectral power density of thermal radiation on the wall surface temperature in the region $3 \mu\text{m}$ under the condition $\varepsilon = 1$. The effect of power of recombination and bremsstrahlung radiation in the Globus-M2 tokamak was estimated for the thickness of plasma layer on the optical path of pyrometer ~ 1 m. For channel $4 \mu\text{m}$, the effect of recombination and bremsstrahlung radiation is less, so it is sufficient to perform calculations for channel $3 \mu\text{m}$. The calculation is given without taking into account impurities in wall plasma. The graph shows that at a plasma temperature of more than 10 eV and moderate density of particles, the wall plasma can be considered transparent to the thermal radiation of surface.

3. Wall temperature measurement in Globus-M2 tokamak area of divertor

Experiments on contactless measurement of surface temperature interacting with plasma were carried out on tokamak Globus-M2 [10]. Radiation was recorded during the study in area of the lower dome of tokamak chamber

near output of outer branch of separatrix. The wall temperature was measured using a pyrometer together with infrared camera. Both instruments were located on outlet with a gate valve with diameter of 40 mm. The combined use of pyrometer and infrared camera made it possible to record both the spatial distribution and the absolute value of surface temperature. Divertor radiation from area with diameter of 20 mm was directed into pyrometer through a sapphire window and rotating aluminum mirror.

The area from which radiation was recorded is shown in Fig. 6. The pyrometer adjustment was performed using a laser. The laser was positioned on axis of lens instead of pyrometer detector unit. This area was located at a radius of 300 mm from the axis of the torus. Temperature measurements were carried out on plateau of current. Discharge parameters of #41152 are shown in Fig. 7. In this experiment the time resolutions of pyrometer and IR camera were 30 and $1000 \mu\text{s}$, respectively. Time resolution of pyrometer was determined by parameters of galvanic isolation installed in the tokamak information collection system. It can be seen that with the appearance of sawtooth oscillations in the plasma, pyrometer and infrared camera recorded flashes of radiation on the wall of the tokamak chamber with different time resolution. The period of these flashes was 3–4 ms, and duration was ~ 2 ms. The maximum wall temperature measured by pyrometer and infrared camera reached 550 and 250°C ,

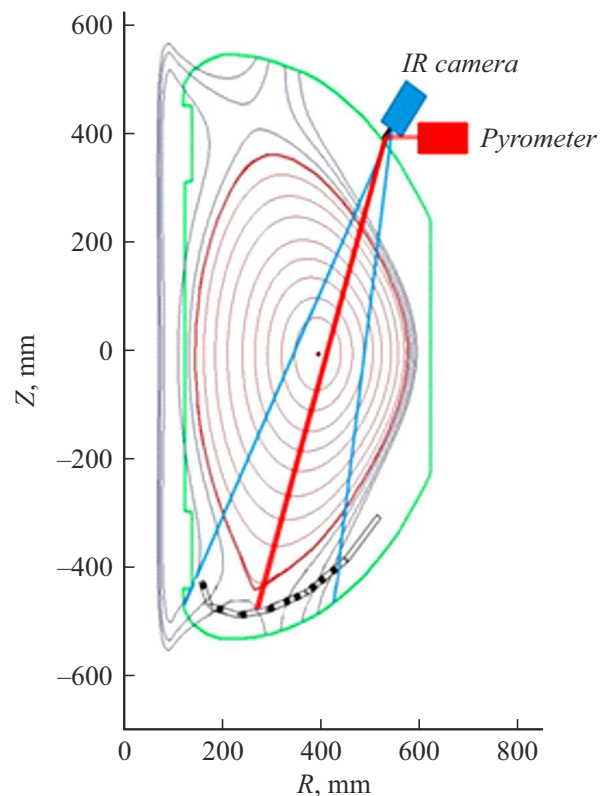


Figure 6. Tokamak area from which the radiation was recorded.

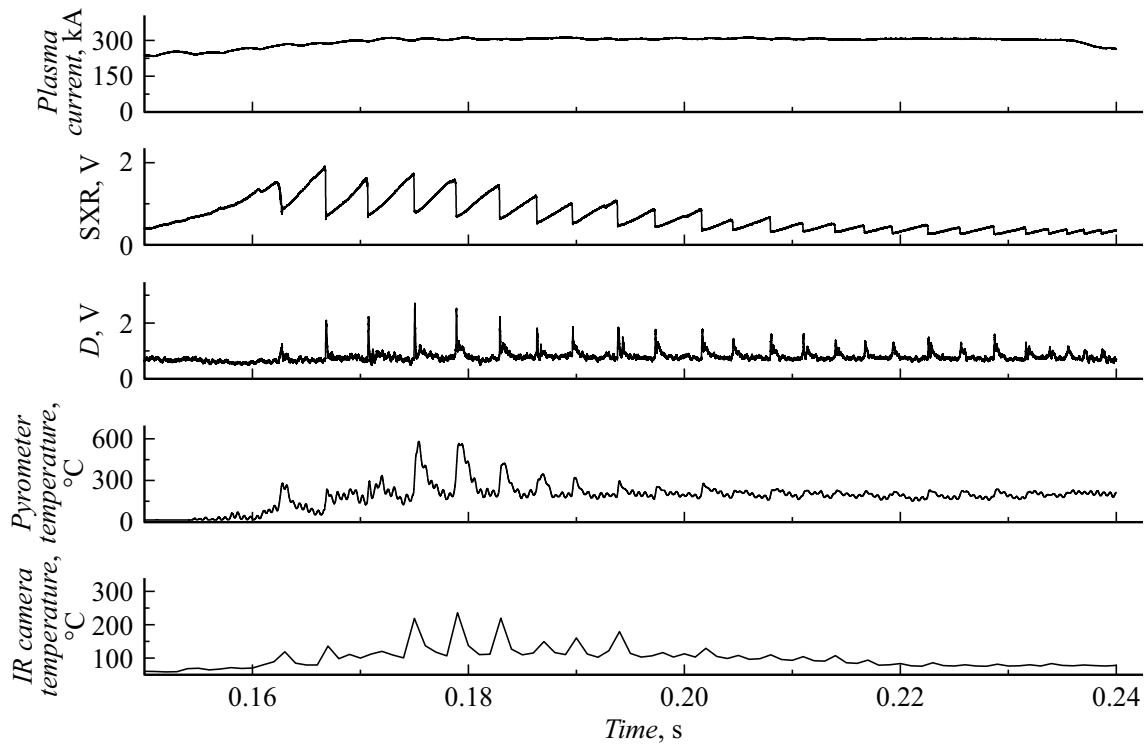


Figure 7. Dependence of discharge parameters #41152 on time.

respectively. It can be assumed that such a discrepancy in measurement was attributable, for example, to the impact of an indefinite value of radiation coefficient characteristic of infrared camera operating in the same spectral range (3.7–4.8 μm).

4. Study of the surface of W-Li composite sample exposed to multiple irradiation with deuterium pulsed plasma

Structural changes on the surface of samples were studied in work [11] under conditions of cyclic exposure to deuterium plasma under energy loads simulating the modes of plasma current disruption in a tokamak. W-Li composite samples were used for the study, they were prepared on the basis of a structure made of pressed tungsten wire with diameter of 0.2 mm and saturated with lithium. A sample of size $20 \times 12 \times 1$ mm was placed at a distance of 220 mm from the plasma jet source in vacuum chamber with a residual pressure 10^{-5} Torr. The samples were heated using a halogen lamp with a power of 35 W to temperature of 200°C , which was controlled by thermocouple. The sample was attached to the heater using a tungsten mask (Fig. 8). The sample was repeatedly irradiated with deuterium plasma on plasma gun test bench [12]. The coaxial plasma gun with pulsed working gas supply had a capacitor storage capacity of $160 \mu\text{F}$

and generated jet of deuterium plasma with duration of $15 \mu\text{s}$. The time between pulses was 60 s. The sample was irradiated with an accumulator voltage of 4 kV, with an energy density of 0.25 MJ/m^2 (with a power density of 22 GW/m^2). In the interval between the pulses, the temperature of front surface of the sample was measured using a two-color ratio pyrometer at wavelengths 3 and $4 \mu\text{m}$. The pyrometer readings were not analyzed during the first $100 \mu\text{s}$ after the initiation of the gun pulse, since dense plasma could distort the thermal radiation emanating from the surface. Temperature was measured after the termination of visible radiation near the sample and during the monotonous decrease of the pyrometer signals after irradiation, i.e without any plasma exposure. The measurement results were reproduced if the sample was changed.

Results of temperature measurements of the sample front surface are shown in Fig. 9. It can be seen that the temperature reached values exceeding 3000°C for a time less than 1 ms, and the duration of decline to a value of 200°C increased with an increase in the number of irradiations and amounted to 200 ms after 70 pulses. It can be assumed that a layer with low thermal conductivity was formed during the irradiation of W-Li surface. The use of a pyrometer under these conditions can be considered as a way to control the formation of heat-insulating films on a surface interacting with plasma.

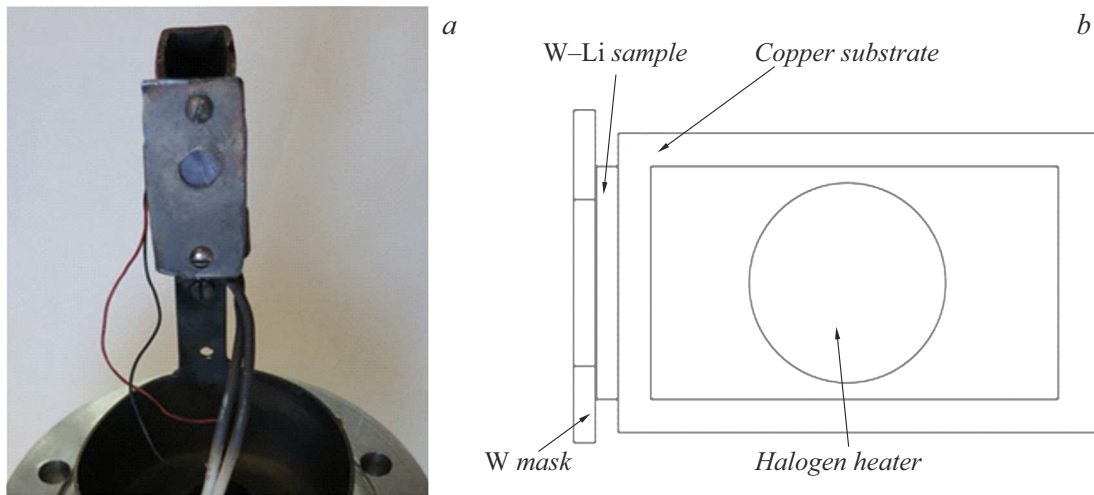


Figure 8. General view (a) and scheme of attachment (b) of the irradiated sample.

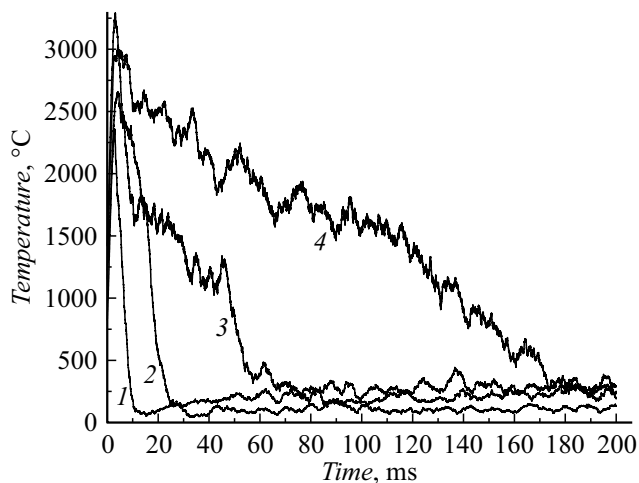


Figure 9. Temperature evolution of front surface of W-Li sample after plasma exposure for a different number of irradiation pulses: 1 — 7, 2 — 29, 3 — 52, 4 — 70. The power density of the plasma jet was 22 GW/m^2 .

Conclusion

A high-speed two-color pyrometer with a time resolution of $2 \mu\text{s}$ has been developed and calibrated. The main factors affecting the measurement of surface temperature in the conditions of its interaction with plasma were analyzed. It was shown that the edge plasma can be considered transparent to thermal radiation at a plasma temperature of more than 10 eV and moderate density of particles. The first experimental studies on non-contact measurement of temperature of the surface interacting with plasma were carried out on Globus-M2 tokamak and plasma gun test bench. Sawtooth temperature oscillations were detected on the wall of tokamak chamber near exit of the outer branch of separatrix. The period of these flashes was 3–4 ms, and

duration was ~ 2 ms. The time resolution and the value of wall temperature measured by a high-speed pyrometer exceeded these values measured by infrared camera. Front surface temperature of the W-Li sample was measured on the plasma gun test bench under the conditions of cyclic action of a deuterium plasma jet under loads simulating the modes of plasma current disruption in a tokamak. The sample temperature reached values exceeding 3000°C in a time less than 1 ms. The thermal conductivity of sample degraded with an increase in the number of irradiations. This was expressed by a progressive decrease in the cooling rate of the target after the pulse. Analysis of the dynamics of changes in the temperature of the surface interacting with the plasma, implemented using a high-speed two-spectral pyrometer, can be considered as a way to control the formation of insulating films on its surface.

Funding

The work was performed using the FCCP „Materials Science and Diagnostics in Advanced Technologies“ (RFMEFI62119X0021 project), which includes a unique scientific installation „Spherical Tokamak Globus-M“. The study was supported by the Ministry of Science and Higher Education of the Russian Federation under the state assignment in the field of science on project № 0784-2020-0020, experimental plasma gun bench for irradiating materials was maintained under the state assignment № 0040-2019-0023, the diagnostics was used on the Globus-M2 tokamak under the state assignment № 0034-2021-0001.

Conflict of interest

The authors declare that they have no conflict of interest.

References

- [1] R.A. Pitts, S. Carpentier, F. Escourbiac, T. Hirai, V. Komarov, S. Lisgo, A.S. Kukushkin, A. Loarte, M. Merola, A. Sashala Naik, R. Mitteau, M. Sugihara, B. Bazylev, P.C. Stangeby. *J. Nuclear Mater.*, **438**, S48 (2013).
- [2] Y. Ueda, J.W. Coenen, G. De Temmerman, R.P. Doerner, J. Linke, V. Philipps, E. Tsitron. *Fusion Engineer. Design*, **89**, 901 (2014).
- [3] N.A. Urzhumtsev, A.V. Voronin, A.A. Kapralov, R.S. Paset, G.Yu. Sotnikova. *Bystrodeystvuyushchij dvukhtsvetnyj pirometr dlya kontrolya temperatury poverkhnosti vo vremya vozdeystviya plazmennoj strui*, XXVI International scientific-technical conference on photoelectronics and night vision devices, Moscow, 25–27 may, 2022), pp. 370–372 (in Russian).
- [4] A. Frunze. *Fotonika*, **4**, 32 (2009) (in Russian).
- [5] G.Yu. Sotnikova, S.A. Alexandrov, G.A. Gavrilov. *Uspekhi prikladnoi fiziki*, **10** (4), 389 (2022) (in Russian).
- [6] L.Z. Kriksunov. *Spravochnik po infrakrasnoj tekhnike* (Sov. Radio, Moscow, 1978), p. 30 (in Russian).
- [7] G.Yu. Sotnikova, G.A. Gavrilov, A.A. Kapralov, K.L. Muratkov, E.P. Smirnova. *Rev. Scientific Instrum.*, **91**, 015119 (2020). DOI: 10.1063/1.5108639
- [8] LLC „IoffeLED“ Ltd, <http://www.ioffeled.com>
- [9] S.Yu. Lukyanov. *Goryachaya plazma i upravlyaemyj yadernyj sintez* (Nauka, M., 1975) (in Russian).
- [10] Yu.V. Petrov, V.K. Gusev, N.V. Sakharov, V.B. Minaev, V.I. Varfolomeev, V.V. Dyachenko, I.M. Balachenkov, N.N. Bakharev, N.N. Bondarchuk, V.V. Bulanin, F.V. Chernyshev, M.V. Iliasova, A.A. Kavin, E.M. Khilkevitch, N.A. Khromov, E.O. Kiselev, A.N. Konovalov, V.A. Kornev, S.V. Krikunov, G.S. Kurskiev, A.D. Melnik, I.V. Mirosnikov, A.N. Novokhatskii, N.S. Zhiltsov, M.I. Patrov, A.V. Petrov, A.M. Ponomarenko, K.D. Shulyatiev, P.B. Shchegolev, A.E. Shevelev, O.M. Skrekel, A.Yu. Telnova, E.A. Tukhmenova, V.A. Tokarev, S.Yu. Tolstyakov, A.V. Voronin, A.Yu. Yashin, P.A. Bagryansky, E.G. Zhilin, V.Yu. Goryainov. *Overview of Globus-M2 Spherical Tokamak Results at the Enhanced Values of Magnetic Field and Plasma Current* (Accepted Manuscript online 17 September 2021), DOI: 10.1088/1741-4326/ac27c7
- [11] A.V. Vertkov, A.V. Voronin, V.G. Gusev, E.V. Demina, I.E. Lyublinsky, V.N. Pimenov, M.D. Prusakova. *Perspektivnye materialy*, **10**, 15 (2018) (in Russian).
- [12] A.V. Voronin, V.K. Gusev, Ya.A. Gerasimenko, Yu.V. Sudinokov. *ZhTF*, **83** (8), 36 (2013) (in Russian).

Translated by A.Akhtyamov